

# VLBA observations of SiO masers: arguments in favor of radiative pumping mechanisms

J.F. Desmurs<sup>1,2</sup>, V. Bujarrabal<sup>1</sup>, F. Colomer<sup>1</sup>, and J. Alcolea<sup>1</sup>

<sup>1</sup> Observatorio Astronómico Nacional (IGN), Apartado 1143, 28800 Alcalá de Henares, Spain (desmurs,bujarrabal,colomer,j.alcolea@oan.es)

<sup>2</sup> Joint Institute for VLBI in Europe, Postbus 2, 7990 AA Dwingeloo, The Netherlands

Received 12 May 1999 / Accepted 6 June 2000

**Abstract.** We have performed VLBA observations of the SiO  $v=1$  and  $v=2$   $J=1-0$  masers in two AGB stars, TX Cam and IRC +10011. We confirm the ring-like spatial distribution, previously found in several AGB objects, as well as the tangential polarization pattern, already reported for TX Cam. Both properties, that seem to be systematic in this kind of objects, are characteristic of radiatively pumped SiO masers. On the contrary, we do not confirm the previous report on the spatial coincidence between the  $J=1-0$   $v=1$  and 2 masers, a result that would have argued in favor of collisional pumping. We find that both lines sometimes arise from nearby spots, typically separated by 1–2 mas, but are rarely coincident. The discrepancy with previous results is explained by the very high spatial resolution of our observations,  $\sim 0.5$  mas, an order of magnitude better than in the relevant previously published experiment.

**Key words:** masers – polarization – techniques: interferometric – stars: AGB and post-AGB – radio lines: stars

## 1. Introduction

SiO maser emission at 7 mm wavelength ( $v=1$  and  $v=2$ ,  $J=1-0$  transitions near 43 GHz) has been observed in AGB stars with very high spatial resolution by means of VLBI techniques, yielding important results in relation with their not yet well understood pumping mechanism. The 7 mm maser emission regions are found to be distributed in a number of spots forming a ring-like structure at about 2–3 stellar radii: see observations of TX Cam, U Her, W Hya, and VX Sgr by Diamond et al. (1994), Miyoshi et al. (1994), and Greenhill et al. (1995). This ring-like flux distribution arises naturally in the framework of the radiative pumping mechanism of SiO masers (see Bujarrabal 1994a, and references therein), that requires a shell-like matter distribution. These structures may also be possible in collisional models, which are practically not geometry dependent (e.g. Doel et al. 1995). From observations with the KNIFE VLBI array, Miyoshi et al. (1994) reported that the emission of these two lines systematically arises from positionally coincident spots, at least as seen with their 7 mas beam. Miyoshi et

al. claimed that this result is a conclusive proof in favor of collisional pumping schemes, since radiative mechanisms, always more selective, tend to require different physical conditions to pump the  $v=1$  and  $v=2$  masers.

VLBA observations (Kemball & Diamond 1997) have also shown that most SiO spots are linearly polarized in the tangential direction, i.e. perpendicularly to the direction to the ring center, in a particularly well defined pattern. This result was interpreted as due to a magnetic field, but uncomfortably strong (close to 10 G). Moreover, Kembal & Diamond found problems to define a distribution of possible field directions that would explain such a tangential pattern, mostly if it systematically applies to SiO masers in AGB stars. The problem of explaining the tangential polarization can be solved invoking radiative pumping. Tangential linear polarization in SiO masers arises in these models as a direct result of the anisotropy introduced by the absorption of stellar (radial) photons, even in the absence of magnetic field. In fact, tangential polarization was predicted from radiative pumping models more than ten years before any VLBA observations were available (Bujarrabal & Nguyen-Q-Rieu 1981; Western & Watson, 1983b).

## 2. Observations and data analysis

We performed observations of the  $v=1$  and  $v=2$ ,  $J=1-0$  lines of SiO (at a rest frequency of 43,122.080 and 42,820.587 MHz respectively) with the NRAO Very Long Baseline Array<sup>1</sup> in April 1996. The system was setup to record 4 MHz of left-circular and right-circular polarizations in both lines. The correlation was produced at the VLBA correlator in Socorro (NM, USA) providing 128 spectral channel cross correlations of the parallel- and cross-hand polarization bands (thus achieving a spectral resolution of  $\sim 0.22$  km s<sup>-1</sup>), out of which all four Stokes parameters could be retrieved, and hence the full polarization state of SiO masers.

The calibration procedure used to derive the total intensity maps followed the standard scheme in the Astronomical Image Processing System (AIPS) for spectral line experiments. Maps of  $50 \times 50$  mas were produced for both  $v=1$  and  $v=2$  lines

<sup>1</sup> The National Radio Astronomy Observatory (NRAO) is operated by Associated Universities, Inc., under cooperative agreement with the National Science Foundation.

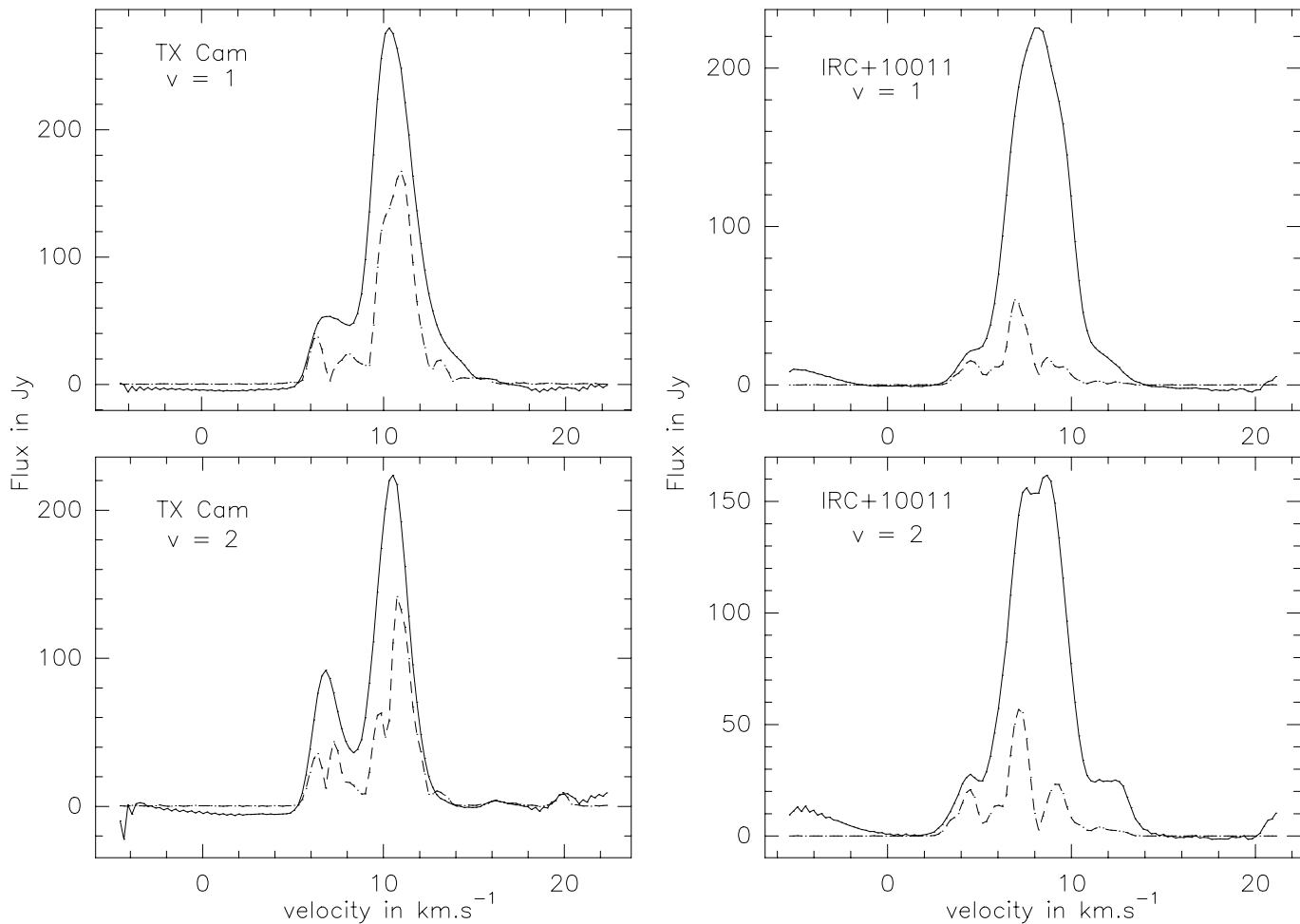


**Fig. 1.** Auto correlation (continuous line) and crosscorrelation (dash) spectrum of TX Cam and IRC +10011 for the  $v=1$  and  $v=2$  masers

separately, with a restoring beam of  $0.6 \times 0.3$  mas FWHM (with the major axis being at a position angle  $PA = -60^\circ$ , measured from North to East) for TX Cam and  $0.7 \times 0.2$  mas ( $PA = -29^\circ$ ) for IRC +10011.

AIPS also provides a set of tools to produce maps of the linearly polarized spectral line emission (for more details see e.g. the AIPS Cookbook<sup>2</sup>, Cotton 1993, Leppanen et al. 1995, and Kemball et al. 1995). We observed the quasar 3C 454.3 (of known linear polarization) to estimate the delay correction between the RCP and LCP bands. The instrumental polarization leakage (or D-terms) were estimated from observations of the unpolarized quasar 3C 84, consistently with the corrections found independently with AIPS from the SiO maser sources.

In Figs. 1, we show the spectrum of auto-correlation and cross-correlation. These spectrum tell us that in the case of TX Cam less than 50% of the flux is lost in our map due to our high spatial resolution, but for IRC +10011, about 75% of the flux is lost. This suggest that the map of IRC +10011 is essentially sensible to the most compact components and that we missed part of flux due to the presence of extended components.

The determination of the absolute polarization position angle for IRC +10011 was performed using single dish observations made at the same epoch with the radio telescope at Centro Astronómico de Yebes (OAN, Spain). We identified and measured the polarization angle of a component spatially isolated within our velocity resolution in our VLBA maps (Desmurs et al. 1999). We measured the absolute position angle of the polarization observed at the same velocity in our single dish data. Comparing both polarization angles, we were able to find the correction to be applied to our VLBI map in order to be in agreement with our single dish observations. We estimate that the confidence in the final position angle is  $\pm 10^\circ$ . We checked also that the correction obtained in this way, applied on the polarization map of 3C 454.3, produced a result consistent with that shown by Kemball et al. (1996).

Maps of the two transitions were independently produced by solving the residual fringes-rates on the line sources. This correction is determined by selecting a channel containing a simple feature with a simple spatial structure and a high S/N ratio (strong emission), that is used as phase reference for all other channels. To do this, we selected a maser spot appearing in both transitions assuming that these spots were actually spa-

<sup>2</sup> The AIPS Cookbook is available at the URL <http://www.cv.nrao.edu/aips/cook.html>

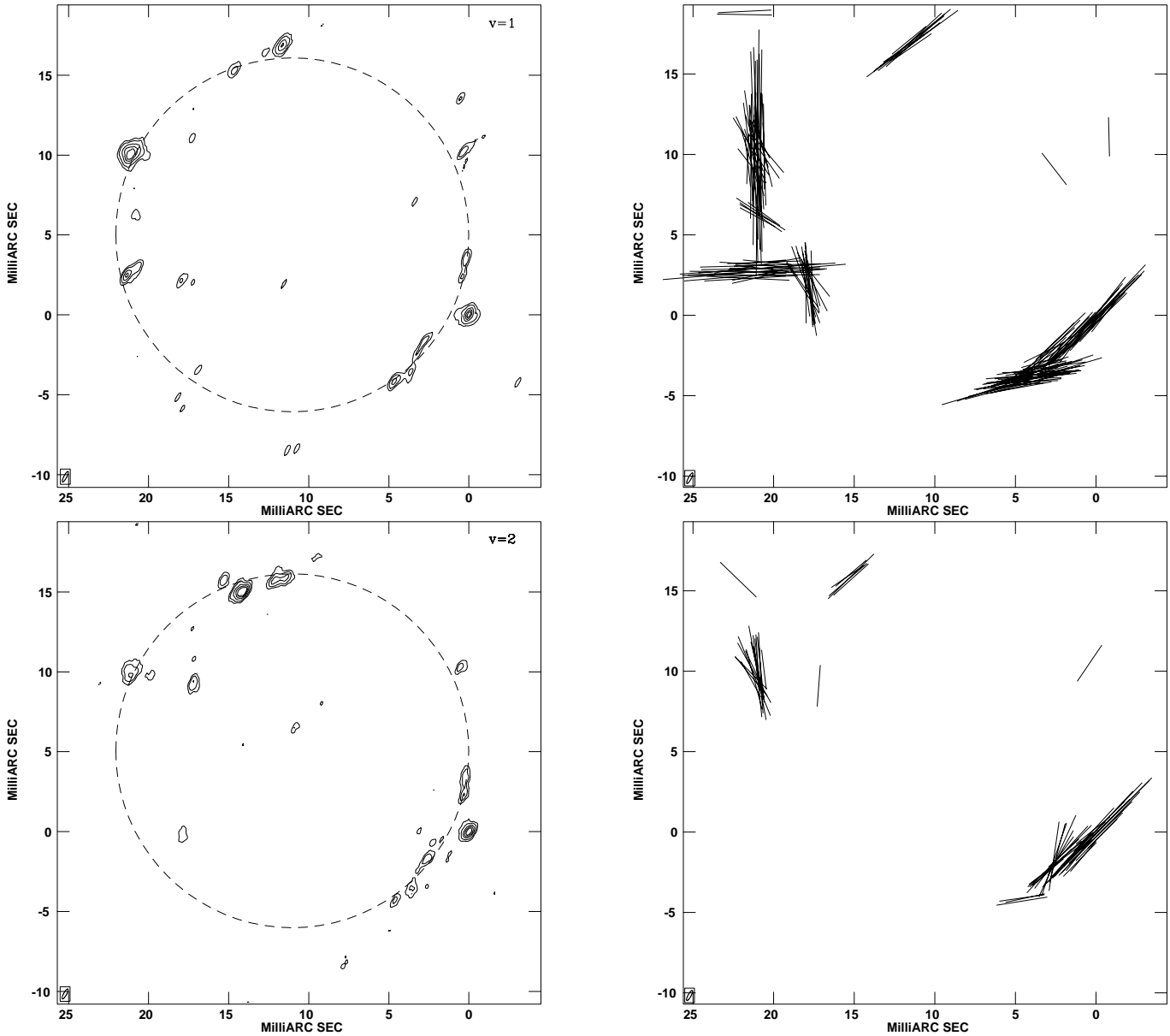


**Fig. 2.** Integrated intensity (left) and polarization maps (right) of the  $v=1$  (top) and  $v=2$  (bottom)  $J=1-0$  lines of SiO towards IRC +10011. Contours are multiples by 10% of the peak flux in each transition (68 Jy and 67 Jy, respectively). The vectors in the linear polarization maps indicate the plane of the electric field vector and their length are scaled as  $1 \text{ mas} \equiv 0.5 \text{ Jy beam}^{-1}$ . The dashed circles are identical and are drawn to ease the comparison of both images

tially coincident. This fixed the position of that maser spots at the map origin in both transitions. This procedure assumes that this maser spot that appears in both lines at the same velocity and position respectively to the rest of the emission distribution actually arises from the same condensation (see result on Figs. 2 and 3); a similar procedure was followed for example, by Miyoshi et al. (1994).

### 3. Results and discussion

Our high-quality VLBA maps (Figs. 2 and 3) confirm that both  $v=1$  and  $v=2$   $J=1-0$  maser transitions arise from ring-like struc-

tures, at a distance from the center  $\sim 11 \text{ mas}$  for IRC +10011, and  $\sim 14 \text{ mas}$  for TX Cam. These radii are equivalent to about  $8 \cdot 10^{13} \text{ cm}$  (assuming a distance of  $\sim 500 \text{ pc}$  for IRC +10011, and  $\sim 350 \text{ pc}$  for TX Cam). In IRC +10011, a well defined pattern of tangential linear polarization is found. Linear polarization degrees as high as 22% are measured, though some spots are not linearly polarized. A tangential polarization pattern has been also detected in TX Cam, consistent with the work published by Kemball et al. (1995), and with similar properties to those of we find in IRC +10011.

The above observational results are expected from theoretical models for SiO radiative pumping. In fact, both the flux

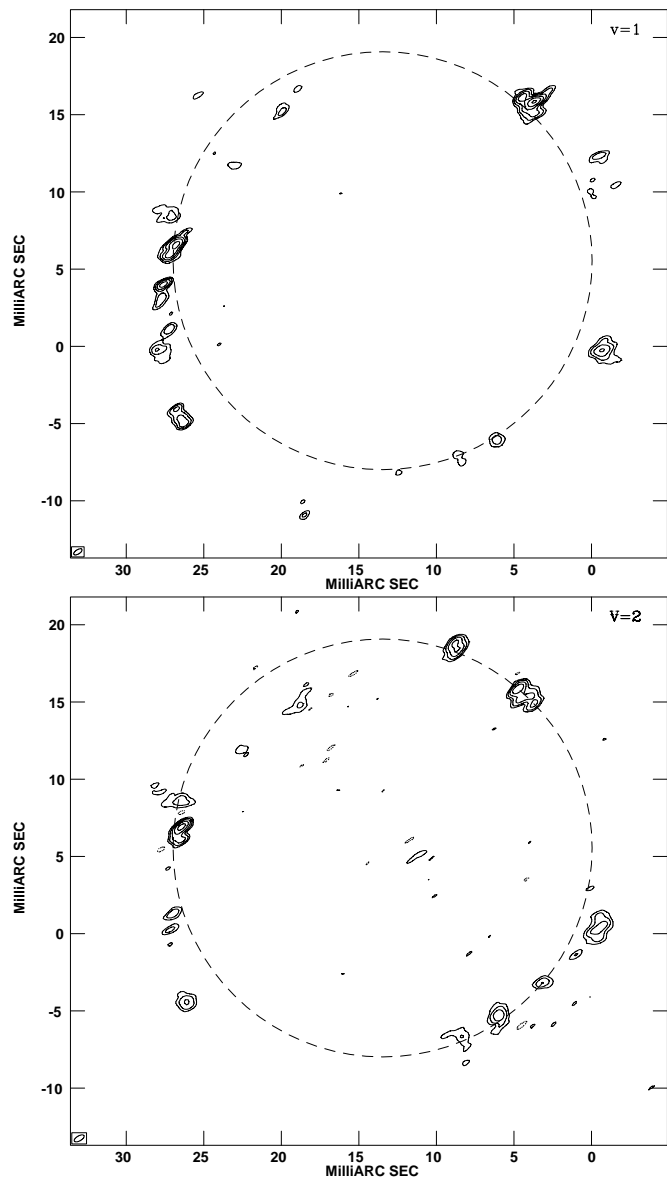


**Fig. 3.** Integrated intensity maps of the  $v=1$  (top) and  $v=2$  (bottom),  $J=1-0$  lines of SiO towards TX Cam. Contours are multiples by 10% of the peak flux in each transition (96 Jy and 72 Jy, respectively). The dashed circles are identical and are drawn to ease the comparison of both images

distribution in a thin ring and the tangential polarization are properties essentially related to the radiative pumping of SiO masers. Excitation of SiO vibrational states by absorption of stellar photons is much more probable than collisional excitation, as one can easily demonstrate by taking into account the expected physical conditions in the emitting regions. For instance, an SiO shell located at 3 stellar radii, with a kinetic temperature of 1500 K and a density of  $10^9$  particules  $\text{cm}^{-3}$ , presents an absorption rate of stellar photons in the  $v=0 \rightarrow 1$  transition that is about 200 times larger than the corresponding collisional excitation rate. However, radiative excitation is efficient to produce population inversion in  $v > 0$  rotational transitions only when

the SiO region fulfills some conditions, particularly when radiation comes from a central source at some distance from the SiO shell (Bujarrabal & Nguyen-Q-Rieu 1981, Bujarrabal 1994a). Under such conditions, the high probability of the photon absorption implies that the pumping must be radiative. Due to the geometrical conditions for the radiative pumping, the radiative maser excitation is more efficient close to the inner boundary of the SiO shell. In terms of flux, this effect is strengthened by the non-linear maser amplification (Bujarrabal 1994b, Western & Watson 1983a). This theoretically indicates that “tangential” (i.e. perpendicular to the radial direction) amplification is dominant, and leads to a radial flux distributions in a thin ring, strikingly similar to that observed in these stars.

Tangential polarization is also expected from radiative pumping models, as can be understood from a semiclassical point of view. Radiation incident on a gas shell from a central source must show electric and magnetic fields perpendicular to the radial direction. Linear molecules are preferentially excited by the absorption of such photons when they rotate in the tangential plane, and will preferentially rotate in it after the excitation. This is expected to be the case when SiO is vibrationally excited from the  $v$  to the  $v+1$  state by absorption of stellar  $8\mu$  photons. In other words, for a given  $J$  level in  $v+1$ , the most populated magnetic sublevels will be those with largest  $|M|$  values (when the quantization of the magnetic quantum number is taken along the radial direction). When the molecular emission is essentially tangential (as for SiO masers), the tangential plane, in which molecules rotate, contains the line of sight for intense spikes: one then expects to detect “tangential polarization”, in agreement with observations. Note that this mechanism does not require any magnetic field or exotic maser saturation effect.

This intuitive explanation of the linear polarization observed in SiO masers was first proposed, to our knowledge, by Bujarrabal & Nguyen-Q-Rieu (1981). Soon later, but well before the first VLBA polarization maps, Western & Watson (1983a,b) developed more in detail the theory of maser polarization under these conditions, confirming the expected presence of strong tangential polarization in the case of SiO masers from evolved stars. We can also see a more recent discussion in Elitzur (1996).

Our maps also show that the  $v=1$  and  $v=2$  spots are systematically not coincident. Positioning of the  $v=1$  features relative to the  $v=2$  ones has been performed as described in Sect. 2. In TX Cam we identify, from the integrated flux maps in Fig. 3, about 17 features in both  $v=1$  and  $v=2$  transitions, out of which only one appears to be spatially coincident, within the resolution of our observation. In the case of IRC +10011, we find about 13 features, 4 of which could be coincident (see Fig. 2). In most cases in which spots of these lines are nearby, there is a systematic shift between them, of about 1–2 mas ( $\sim 10^{13}$  cm), being the  $v=2$  ones placed in a layer slightly closer to the star (Figs. 4 and 5).

The way how the maps in the two lines are aligned (see Sect. 2) implies that at least one maser spot appears in both lines at the same spatial position respectively to the rest of the emission distribution. Nevertheless, we can easily check that

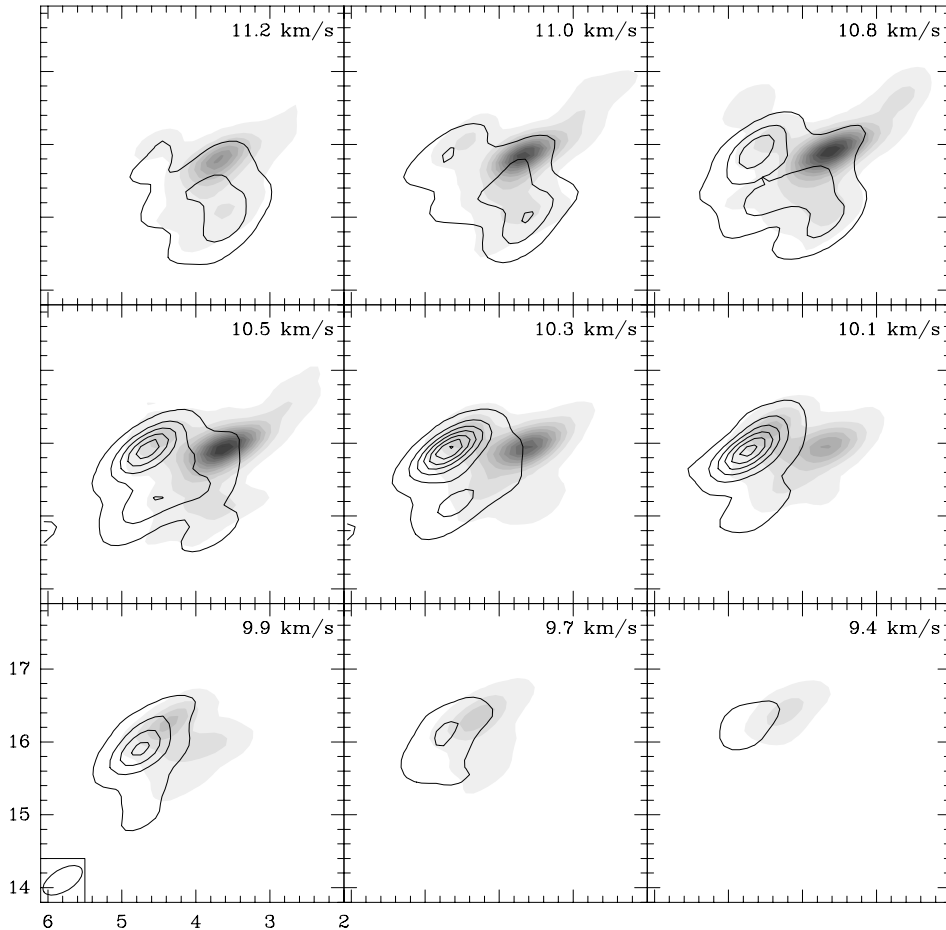


**Fig. 4.** Intensity channel map of the maser features at a position offset of (5, 15) mas in TX Cam, displaying the difference in position that is systematically observed between the  $v=1$  (towards the west, level in grey) and  $v=2$  emission (towards the east, contour levels, see text). Lowest contour is 5% of the flux peak (25 Jy/beam)

there is no possibility of selecting any spot that permits the alignment of a majority of the other spots in both lines.

Another geometrical argument is that the diameters of both emission rings differ. After summing all the velocity channels into one velocity integrated map (Figs. 2 and 3), we determined the position of the maser spots showing a S/N ratio at least equal to  $5\sigma$  (for TX Cam  $1\sigma$  is  $\sim 0.86$  Jy and for IRC +10011  $1\sigma$  is  $\sim 0.7$  Jy). We fitted a ring shell to our data giving a relative weight to each maser spot proportional to its intensity. The parameters (position center and radius of the emission ring) for which the coefficient of standard deviation is minimum is kept as the best possible fitting. As a result, for TX Cam the radii found for the  $v=1$  and  $v=2$  maser transition are respectively  $14.5 \pm 0.2$  mas and  $13.2 \pm 0.2$  mas. This represents a difference between both diameters of the emission rings of  $2.6 \pm 0.5$  mas, to be compared with our beam resolution of  $0.6 \times 0.3$  mas. For IRC +10011, the radii found are  $11.7 \pm 0.2$  mas for the  $v=1$  and  $11.1 \pm 0.2$  mas for the  $v=2$ , which gives a diameter difference of  $1.2 \pm 0.5$  mas, for a resolution beam of about  $0.7 \times 0.2$  mas. These differences in the maser ring sizes are significant enough in comparison with our beam resolution, which leads us to conclude that the two lines come from shells with significantly different diameters.

The conclusion that the  $v=1$  and  $v=2$  masers arise from the spatially coincident spots obtained previously by Miyoshi et al. (1994) is then not confirmed by our higher-resolution data.

This disagreement could be explained by the fact that the measured shifts are significantly smaller than the beam in their data (7 mas). The claim by these authors ruling out radiative pumping, on the basis that radiative models tend to require different conditions for the pumping of transitions in these two vibrational states (see Sect. 1), was clearly premature. In fact, the systematic separation between the  $v=1$  and  $v=2$  spots in our data must be considered as an additional support for the radiative pumping.

Preliminary calculations for radiatively pumped models (see Bujarrabal 1994a and Herpin 1998) indicate that, when both  $v=1$  and 2 masers appear in the same clump, the  $v=2$  lines tend to select its innermost parts, in agreement with the data. In any case, published calculations have not explicitly addressed this important point yet, and new accurate calculations are required.

Our observational results could also be explained under certain condition by collisional pumping. The tangential polarization can be produced in the presence of strong magnetic fields within certain directions, independently of the pumping process. But this mechanism cannot explain the tangential polarization if it is (as it seems) a systematic property in evolved stars. For instance, Kembell & Diamond (1997) argue that a pattern like that detected in TX Cam by them would require a poloidal magnetic field with a non-arbitrary inclination of the pole with respect to the plane of the sky,  $\sim 40^\circ$ – $60^\circ$ , other angles even leading to radial polarization. Shell-like spatial distributions of the

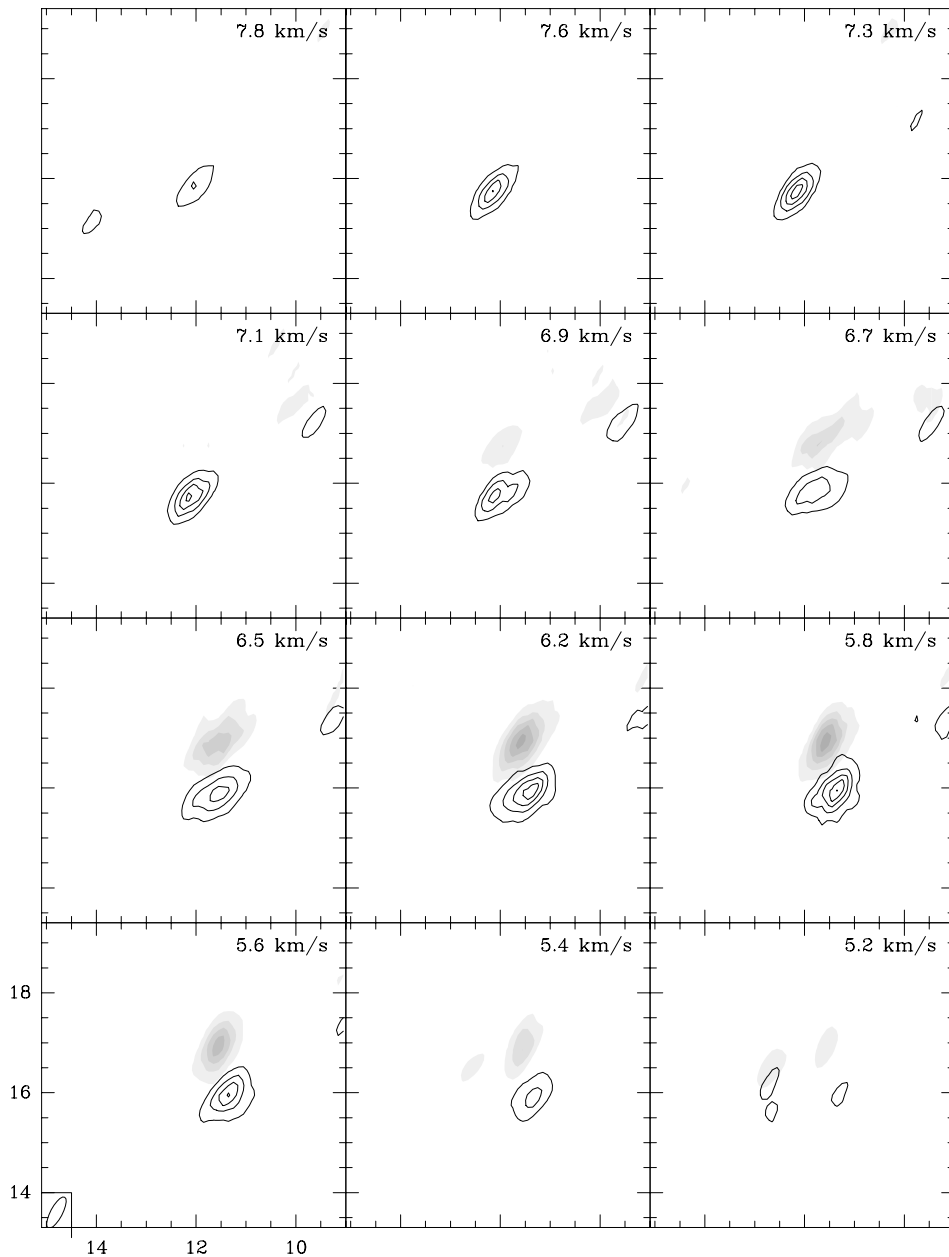


**Fig. 5.** Same as Fig. 4, but for the maser features at a position offset of (+12, +16) mas in IRC +10011. Lowest contour is 5% of the flux peak (11.5 Jy/beam)

maser flux can also appear when the pumping is collisional, if it acts in certain pulsating atmospheres (Humphreys et al. 1996, Doel et al. 1995). As we have mentioned, the collisional pumping models tend to predict spatial coincidence between the  $v=1$  and  $v=2$  masers, though in the above mentioned papers there are also examples in which the  $v=2$   $J=1-0$  masers are placed closer to the star.

But the main conclusion from the discussion presented in this paper is that the bulk of the existing empirical results on SiO maser emission from evolved stars strongly support radiative pumping. The spatial shell-like distribution of the flux, the tangential polarization pattern of  $v=1$  and 2  $J=1-0$  SiO masers, and the shift in their spatial distributions (properties very often found in the existing observations) are intrinsically related with the radiative pumping schemes. Indeed, radiative models

predicted, well before the observations were made, that such properties should be systematically observed.

*Acknowledgements.* We thank an anonymous referee for helpful comments that improved the manuscript. This work has been partially supported by the Spanish DGES Project PB96-0104. JFD acknowledges support for his research by the European Union under contract ERBFMGECT950012.

## References

- Bujarrabal V., Nguyen-Q-Rieu, 1981, A&A 102, 65
- Bujarrabal V., 1994a, A&A 285, 953
- Bujarrabal V., 1994b, A&A 285, 971
- Cotton W.D., 1993, AJ 106, no. 3, 1241
- Desmurs J.F., Bujarrabal V., Colomer F., Alcolea J., 1999, In: Garrett M.A.G., Campbell R., Gurvits L.I. (eds.) EVN/JIVE VLBI Sym-

- posium No. 4, *New Astronomy Reviews*. Elsevier Science B.V., Amsterdam
- Diamond P.J., Kemball A.J., Junor W., et al., 1994, *ApJ* 430, L61
- Doel R.C., Gray M.D., Humphreys E.M.L., Braithwaite M.F., Field D., 1995, *A&A* 302, 797
- Elitzur M., 1996, *ApJ* 457, 415
- Greenhill L.J., Colomer F., Moran J.M., et al., 1995, *ApJ* 449, 365
- Herpin F., 1998, Ph.D. Thesis, Univ. de Bordeaux, France
- Humphreys E.M.L., Gray M.D., Yates J.A., et al., 1996, *MNRAS* 282, 1359
- Kemball A.J., Diamond P.J., Cotton, W.D., 1995, *A&AS* 110, 383
- Kemball A.J., Diamond P.J., Pauliny-Toth I.I.K., 1996, *ApJ* 464, L55
- Kemball A.J., Diamond P.J., 1997, *ApJ* 481, L111
- Leppanen K.J., Zensus J.A., Diamond P.J., 1995, *AJ* 110, 2479
- Miyoshi M., Matsumoto K., Kamenno S., Takaba H., Iwata T., 1994, *Nat* 371, 395
- Western L.R., Watson W.D., 1983a, *ApJ* 274, 195
- Western L.R., Watson W.D., 1983b, *ApJ* 275, 195